JAMA Neurology | Original Investigation

Association of In Vivo [^{18}F]AV-1451 Tau PET Imaging Results With Cortical Atrophy and Symptoms in Typical and Atypical Alzheimer Disease

Chenjie Xia, MD; Sara J. Makaretz, BS; Christina Caso, BS; Scott McGinnis, MD; Stephen N. Gomperts, MD, PhD; Jorge Sepulcre, MD, PhD; Teresa Gomez-Isla, MD; Bradley T. Hyman, MD; Aaron Schultz, PhD; Neil Vasdev, PhD; Keith A. Johnson, MD; Bradford C. Dickerson, MD

IMPORTANCE Previous postmortem studies have long demonstrated that neurofibrillary tangles made of hyperphosphorylated tau proteins are closely associated with Alzheimer disease clinical phenotype and neurodegeneration pattern. Validating these associations in vivo will lead to new diagnostic tools for Alzheimer disease and better understanding of its neurobiology.

OBJECTIVE To examine whether topographical distribution and severity of hyperphosphorylated tau pathologic findings measured by fluorine 18–labeled AV-1451 ([^{18}F]AV-1451) positron emission tomographic (PET) imaging are linked with clinical phenotype and cortical atrophy in patients with Alzheimer disease.

DESIGN, SETTING, AND PARTICIPANTS This observational case series, conducted from July 1, 2012, to July 30, 2015, in an outpatient referral center for patients with neurodegenerative diseases, included 6 patients: 3 with typical amnesic Alzheimer disease and 3 with atypical variants (posterior cortical atrophy, logopenic variant primary progressive aphasia, and corticobasal syndrome). Patients underwent [^{18}F]AV-1451 PET imaging to measure tau burden, carbon 11–labeled Pittsburgh Compound B ([^{11}C]PiB) PET imaging to measure amyloid burden, and structural magnetic resonance imaging to measure cortical thickness. Seventy-seven age-matched controls with normal cognitive function also underwent structural magnetic resonance imaging but not tau or amyloid PET imaging.

MAIN OUTCOMES AND MEASURES Tau burden, amyloid burden, and cortical thickness.

RESULTS In all 6 patients (3 women and 3 men; mean age 61.8 years), the underlying clinical phenotype was associated with the regional distribution of the [^{18}F]AV-1451 signal. Furthermore, within 68 cortical regions of interest measured from each patient, the magnitude of cortical atrophy was strongly correlated with the magnitude of [^{18}F]AV-1451 binding (3 patients with amnesic Alzheimer disease, $r = -0.82$; $P < .001$; $r = -0.70$; $P < .001$; $r = -0.58$; $P < .001$; and 3 patients with nonamnesic Alzheimer disease, $r = -0.51$; $P < .001$; $r = -0.63$; $P < .001$; $r = -0.70$; $P < .001$), but not of [^{11}C]PiB binding.

CONCLUSIONS AND RELEVANCE These findings provide further in vivo evidence that distribution of the [^{18}F]AV-1451 signal as seen on results of PET imaging is a valid marker of clinical symptoms and neurodegeneration. By localizing and quantifying hyperphosphorylated tau in vivo, results of tau PET imaging will likely serve as a key biomarker that links a specific type of molecular Alzheimer disease neuropathologic condition with clinically significant neurodegeneration, which will likely catalyze additional efforts to develop disease-modifying therapeutics.

Editorial page 390

Supplemental content

Author Affiliations: Author affiliations are listed at the end of this article.

Corresponding Author: Bradford C. Dickerson, MD, Frontotemporal Disorders Unit, Department of Neurology, Massachusetts General Hospital and Harvard Medical School, 149 13th St, Ste 2691, Charlestown, MA 02129 (brad.dickerson@mgh.harvard.edu).

JAMA Neurol. 2017;74(4):427-436. doi:10.1001/jamaneurol.2016.5755
Published online February 20, 2017.

Alzheimer disease (AD), with amyloid-β neuritic plaques and tau neurofibrillary tangles as hallmark pathologic changes, has diverse clinical manifestations, from typical amnesic disease to atypical variants including a behavioral and dysexecutive variant, posterior cortical atrophy (PCA), logopenic variant primary progressive aphasia (lvPPA), and corticobasal syndrome (CBS).[1] Although fibrillar amyloid plaques are necessary for a pathologic diagnosis of AD,[2] their density and distribution postmortem are weakly associated with clinical features and are not associated with markers of neurodegeneration.[3,4] This finding has been further confirmed in vivo using amyloid positron emission tomographic (PET) imaging.[5] In contrast, postmortem neurofibrillary tangles are closely linked to clinical phenotype and regional neurodegeneration in both typical[3,4] and atypical AD.[6-8] With the recent development of PET ligands specifically labeling the hyperphosphorylated paired helical filament tau pathologic condition present in AD,[9] we can now test the hypotheses regarding associations of tau localization and density with clinical features of AD in vivo.

We performed a detailed clinical and trimodal imaging study, using fluorine 18–labeled AV-1451 ([18F]AV-1451) PET scan, carbon 11–labeled Pittsburgh Compound B ([11C]PiB) PET scan, and structural magnetic resonance imaging (MRI), of 6 patients with biomarker evidence of AD pathologic conditions, 3 of whom have a typical amnesic AD syndrome, and 3 of whom have atypical clinical syndromes, including PCA, lvPPA, and CBS. We hypothesized that clinical phenotype of patients with typical and atypical AD will be associated with the topography of cortical tau but not amyloid pathologic conditions, as measured by [18F]AV-1451 and [11C]PiB tracers, respectively. We further hypothesized that the [18F]AV-1451 signal will better colocalize with atrophy and the severity of the [18F]AV-1451 signal will be better associated with the magnitude of atrophy compared with the [11C]PiB signal.

Key Points

Question How are in vivo tau pathologic findings measured by fluorine 18–labeled AV-1451 ([18F]AV-1451) positron emission tomographic imaging associated with clinical phenotype and atrophy pattern in patients with Alzheimer disease?

Findings In this case series, the underlying clinical phenotype in both patients with typical and atypical Alzheimer disease variants was associated with the regional distribution of the [18F]AV-1451 signal. The localization and magnitude of cortical atrophy was also associated closely with that of [18F]AV-1451 binding.

Meaning These findings provide further evidence that distribution of in vivo tau burden as seen on results of the [18F]AV-1451 positron emission tomographic imaging is a valid marker of clinical symptoms and neurodegeneration for Alzheimer disease.

Methods

Participants

This study was conducted from July 1, 2012, to July 30, 2015. Six patients were recruited from the Massachusetts Frontotemporal Disorders Unit and Alzheimer Disease Research Center Early Onset Dementia Longitudinal Cohort. Each patient's diagnosis was made or confirmed by a behavioral neurologist (B.C.D.) after a comprehensive evaluation, as described previously.[10] Patients 1, 2, and 3 met diagnostic criteria for typical amnesic multidomain probable AD dementia with executive dysfunction. Patients 1 and 2 also exhibited mild visual constructional impairment. Medial temporal lobe and lateral temporoparietal atrophy was present on visual inspection of MRI results for patients 1, 2, and 3.[11] Patient 4 met criteria for PCA, with an initial and progressive cortical visual disturbance (Balint syndrome on results of neurologic examination) in the absence of memory loss, along with alexia, agraphia, and limb apraxia; right lateralized biparietal atrophy was present on visual inspection of MRI results.[12,13] Patient 5 met criteria for lvPPA, with variably fluent speech and impairments in lexical retrieval and phonologic errors in spontaneous speech and on confrontation naming, impaired repetition of phrases, and spared single word comprehension, motor speech, and grammar, with spared episodic memory and visual function; left lateralized posterolateral temporal and inferior parietal atrophy was present on visual inspection of MRI results.[14] Patient 6 met criteria for CBS, with mild left limb rigidity, dystonia, and myoclonus, moderate limb apraxia greater on the left side than right side, a moderate bilateral cortical sensory deficit greater on the left side than right side, and alien limb of the left arm, whereby the left arm moved without voluntary control; right-lateralized perirolandic atrophy was present on visual inspection of MRI results.[15] The **Table** summarizes demographic and clinical data of the patients. This study was approved by the institutional review board of Partners Healthcare, Boston, Massachusetts. All participants gave written informed consent in accordance with guidelines established by the Partners Human Research Committee.

Seventy-seven age-matched controls with normal cognitive function (mean [SD] age, 63.0 [2.7] years; 41 women and 36 men) from the Massachusetts Alzheimer Disease Research Center Longitudinal Cohort also underwent a structural MRI (these individuals did not undergo tau or amyloid PET imaging). Individuals in this cohort were determined to have normal cognitive function with no significant neurologic or psychiatric history after a detailed clinical evaluation by a neurologist or psychiatrist, neuropsychological testing, and a consensus conference (all individuals have the following characteristics: Clinical Dementia Rating score, 0; Mini-Mental State Examination score, ≥28; no neurologic or psychiatric history).

Neuroimaging Data Acquisition and Analysis

Magnetic Resonance Imaging

All participants (patients and controls) underwent a structural MRI scan (Siemens TIM Trio 3.0T; Siemens Medical Systems). The MRI analysis methods used have been previously described in detail, including processing of cortical thickness and spherical registration to align participants' cortical surfaces (Freesurfer 5.3; http://surfer.nmr.mgh.harvard.edu).[10]

Table. Patient Demographic and Clinical Characteristics

Characteristic	Age, y/Sex	MMSE Score	CDR Score	PiB (FLR DVR)[a]	CSF[b] Aβ1-42, pg/mL	CSF[b] t-tau, pg/mL	CSF[b] p-tau, pg/mL	CSF[b] ATI
Patient 1: amnesic AD dementia	50s/Male	15/30	1	1.6	243.5	560.8	75.0	0.27
Patient 2: amnesic AD dementia	60s/Male	22/30	1	1.6	306.1	526.5	79.3	0.36
Patient 3: amnesic AD dementia	60s/Female	25/30	1	1.6	513.4	551.5	86.7	0.58
Patient 4: PCA	60s/Male	[c]	0.5	1.8	[d]	[d]	[d]	[d]
Patient 5: lvPPA	60s/Female	25/30	0.5	1.9	317.7	608.3	72.6	0.33
Patient 6: CBS	60s/Female	27/30	0.5	1.8	218.8	670.9	82.1	0.21

Abbreviations: Aβ1-42, β-amyloid 1-42; AD, Alzheimer disease; ATI, Aβ1-42 tau index; CBS, corticobasal syndrome; CDR, Clinical Dementia Rating; FLR DVR, distribution volume ratio of FLR region (ie, frontal, lateral parietal and temporal, and retrosplenial cortices); CSF, cerebrospinal fluid; lvPPA, logopenic variant primary progressive aphasia; MMSE, Mini-Mental State Examination; PCA, posterior cortical atrophy; PiB, Pittsburgh compound B; p-tau, phosphor-tau; t-tau, total tau.

[a] An FLR DVR greater than 1.2 is consistent with positive fibrillary brain amyloid.

[b] Aβ1-42 levels less than 500 pg/mL is consistent with amyloid plaque pathologic findings; t-tau levels greater than 300 pg/mL and p-tau levels greater than 61 pg/mL are consistent with neurofibrillary tangle pathologic findings.

[c] Patient 4 did not undergo MMSE.

[d] Patient 4 did not undergo CSF testing.

PET Imaging

All 6 patients also underwent [18F]AV-1451 and [11C]PiB PET imaging. [18F]AV-1451 was prepared at Massachusetts General Hospital, with a mean (SD) radiochemical yield of 14% (3%) and mean (SD) specific activity of 216 (60) GBq/μmol (5837 [1621] mCi/μmol) at the end of synthesis (60 minutes), and validated for human use.[16] [11C]PiB was prepared as described previously,[17] with minor modifications. All PET data were acquired using a Siemens/Control Technical Inc ECAT HR+ scanner (3D mode; 63 image planes; 15.2-cm axial field of view; 5.6-mm transaxial resolution and 2.4-mm slice interval). [18F]AV-1451 PET images were acquired from 80 to 100 minutes after a mean (SD) 10.0 (1.0)-mCi bolus injection in 4 × 5-minute frames (to convert millicuries to megabecquerels, multiply by 37). [11C]PiB PET images were acquired with an 8.5- to 15-mCi bolus injection followed immediately by a 60-minute dynamic acquisition in 69 frames (12 × 15 seconds, 57 × 60 seconds). Data from the PET imaging were reconstructed and attenuation was corrected, and each frame was evaluated to verify adequate count statistics and absence of head motion.

To evaluate the anatomy of cortical [18F]AV-1451 and [11C]PiB binding, each patient's PET image data set was rigidly coregistered to the patient's MRI MPRAGE data using SPM8 (Wellcome Department of Cognitive Neurology, Function Imaging Laboratory). The cortical regions of interest (ROIs) defined by the FreeSurfer (http://surfer.nmr.mgh.harvard.edu) parcellation were transformed into the PET imaging native space and PET image data were sampled within each ROI. Similar to a previous report,[18] [18F]AV-1451 specific binding was expressed in FreeSurfer ROIs as the standardized uptake value ratio (SUVR) using the cerebellar gray matter ROI as a reference. [11C]PiB PET data were expressed in FreeSurfer ROIs as the distribution volume ratio (DVR) with the cerebellar gray ROI as a reference,[19] where regional time-activity curves were used to compute regional DVRs for each ROI using the Logan graphical method applied to data from 40 to 60 minutes after injection.[20] Data from the PET imaging were not partial volume corrected.

Neuroimaging Data Analysis

To visually compare the distribution of cortical thickness with that of PET imaging tracer uptake, we created individual maps for atrophy as well as [18F]AV-1451 and [11C]PiB tracer uptake for each patient. For the atrophy map, we performed a whole-cortex general linear model analysis using FreeSurfer,[21] which compares the thickness of the individual patient's cortex at each vertex point across the entire cortical mantle with the thickness of the group of 77 healthy controls. To facilitate within- and between-participant comparison, we displayed—as the minimum and maximum threshold—the 50th and 95th percentile values of the difference in cortical thickness between the patient and healthy controls for a given vertex, where higher values indicate that the patient's cortex is thinner than that of controls, with a magnitude in millimeters represented by the color scale. Similarly, the 50th and 95th percentile [18F]AV-1451 SUVR and [11C]PiB DVR values of each patient were also selected as the minimum and maximum thresholds displayed on their own respective reconstructed cortical surfaces for each PET imaging modality. We chose to display values between the 50th and 95th percentile as they enable comparison of regional differences in atrophy and [18F]AV-1451 and [11C]PiB binding between patients at different stages of disease.

To quantitatively compare cortical thickness with [18F]AV-1451 and [11C]PiB tracer uptake within each patient, 34 ROIs per hemisphere were derived from the Desikan atlas automated cortical parcellation.[22] For each ROI in each patient, we extracted mean [18F]AV-1451 SUVR, mean [11C]PiB DVR, and a standardized z score representing the magnitude of cortical thickness within the ROI normalized to that of the healthy con-

Figure 1. Regional Distributions of Tau, Atrophy, and Amyloid in Patients With Typical Alzheimer Disease (AD)

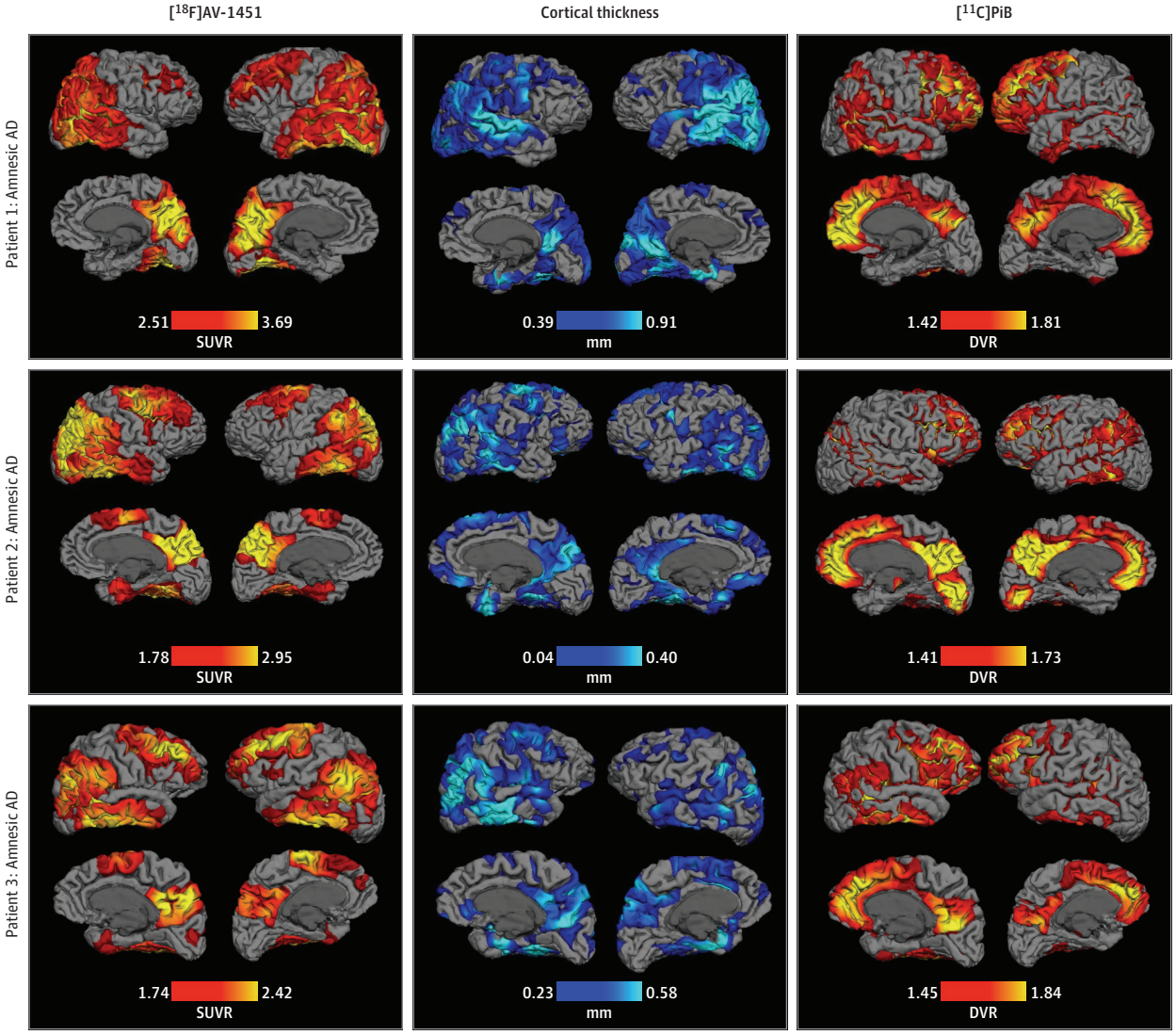

The thresholds selected represent the 50th (minimum) and 95th (maximum) percentile values for each imaging modality for each patient. [11C]PiB indicates carbon 11–labeled Pittsburgh Compound B; DVR, distribution volume ratio; [18F]AV-1451, fluorine 18–labeled AV-1451; and SUVR, standardized uptake value ratio.

trol sample ([patient cortical thickness - $\mu_{\text{age-matched controls}}$]/$\sigma_{\text{age-matched controls}}$). For each patient, Pearson correlation analyses (IBM SPSS Statistics, version 21; IBM Corp) were performed for all ROIs to assess the associations between [18F]AV-1451 SUVR values and cortical thickness (atrophy) *z* scores, and then between [11C]PiB DVR values and atrophy *z* scores.

Results

In cases of typical amnesic AD dementia, high [18F]AV-1451 tracer uptake was seen bilaterally in the posterior cingulate, precuneus, lateral temporoparietal, and occipital cortices (**Figure 1**). In all 3 patients, primary visual, auditory (not shown), and sensorimotor cortices were spared. In patient 1 (with the most advanced disease of all patients, likely Braak stage VI), the global signal was so high that the thresholds for visualization were higher than those that would show a medial temporal cortical signal (eTable in the Supplement displays [18F]AV-1451 SUVR values of select ROIs for all 6 patients). Patients 2 and 3 also showed elevated medial temporal cortical signals. In both patients 2 and 3, high [18F]AV-1451 tracer uptake was also seen in the bilateral dorsolateral prefrontal cortex. These distributions are consistent with Braak stage V neurofibrillary pathologic findings.[23] Closely paralleling [18F]AV-1451 tracer uptake, cortical atrophy was most prominent in the bilateral medial temporal, posterior cingulate, precuneus, lateral temporoparietal, and occipital cortices in all 3 patients. The bilateral dorsolateral prefrontal cortex also showed prominent and moderate atrophy in patients 2 and 3, respectively.

Figure 2. Regional Distributions of Tau, Atrophy, and Amyloid in Patients With Atypical Alzheimer Disease

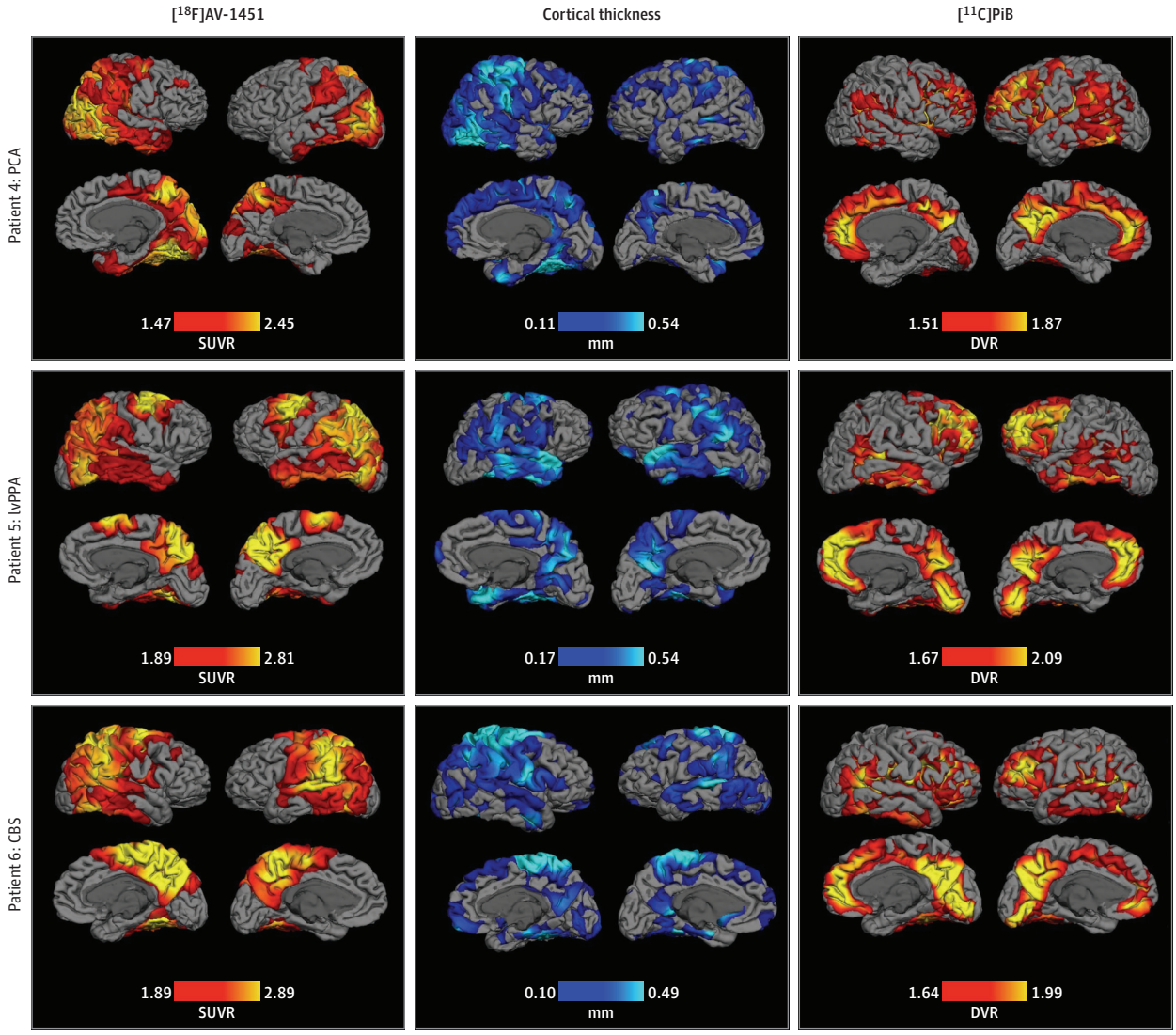

The thresholds selected represent the 50th (minimum) and 95th (maximum) percentile values for each imaging modality for each patient. CBS indicates corticobasal syndrome; [11C]PiB, carbon 11–labeled Pittsburgh Compound B; DVR, distribution volume ratio; [18F]AV-1451, fluorine 18–labeled AV-1451; lvPPA, logopenic variant primary progressive aphasia; PCA, posterior cortical atrophy; and SUVR, standardized uptake value ratio.

In contrast, [11C]PiB tracer uptake was most pronounced in the bilateral medial prefrontal cortex for all 3 patients, where little to no cortical atrophy had been observed, and in the posteromedial cortex, the spatial pattern commonly seen in patients with AD dementia.[24]

In the patients with atypical clinical AD syndromes, high [18F]AV-1451 tracer uptake was seen in a pattern associated with the clinical syndrome and distinct from that of typical AD (**Figure 2**). In patient 4 (diagnosis of PCA), high [18F]AV-1451 tracer uptake was seen most prominently in the occipitoparietal and occipitotemporal visual association areas laterally and medially, with an asymmetric signal that was higher in the right hemisphere, extending into the calcarine fissure and onto the postcentral gyrus. Cortical atrophy was also present in many of these same regions, with right lateralization. The [11C]PiB tracer uptake pattern was distinct from that of [18F]AV-1451 and cortical atrophy, being most pronounced in the left parietal and bilateral medial prefrontal cortices. In patient 5 (diagnosis of lvPPA), [18F]AV-1451 uptake was left lateralized in the left parietal and posterior temporal cortices, and seen in the bilateral posterior dorsolateral prefrontal and precuneus cortices. Cortical atrophy was present with a similar topography, including left lateralized parietal atrophy, albeit with an area of atrophy in the right anterior temporal cortex. Although [11C]PiB uptake was seen in the bilateral medial occipital and parietal cortices, it was most pronounced and extensive in the bilateral medial prefrontal cortices. Finally, in patient 6 (diagnosis of CBS), both high [18F]AV-1451 tracer uptake and prominent cortical atrophy were seen in the bilateral primary and association sensorimotor (perirolandic) cortices, with the right lat-

eralization in accordance with the patient's predominantly left-sided symptoms. In contrast, no [11C]PiB tracer uptake was seen in these areas; instead, it was most notable in the right medial prefrontal and bilateral medial occipitoparietal cortices. These findings support our hypotheses that the [18F]AV-1451 signal localizes in a manner consistent with clinical phenotype and colocalizes with atrophy.

Pearson correlation analyses across the 68 cortical ROIs (34 per hemisphere) support our hypothesis that the intensity of [18F]AV-1451 tracer uptake as seen on PET imaging correlates strongly with the magnitude of atrophy, and support a lack of correlation between the regional intensity of [11C]PiB tracer uptake and the magnitude of cortical atrophy. For each of the 3 patients with typical amnesic AD, [18F]AV-1451 tracer SUVR within a given ROI correlated strongly with the cortical thickness *z* score (patient 1, $r = -0.82$; $P < .001$; patient 2, $r = -0.70$; $P < .001$; and patient 3, $r = -0.58$; $P < .001$), such that ROIs with the highest [18F]AV-1451 tracer uptake were also the ROIs with the most atrophy. In contrast, [11C]PiB uptake was not associated with cortical thickness (patient 1, $r = 0.23$; $P = .07$; patient 2, $r = -0.003$; $P = .98$; and patient 3, $r = -0.17$; $P = .15$). **Figure 3** provides scatterplots to illustrate the associations between regional values of [18F]AV-1451, [11C]PiB, and cortical thickness for the 3 patients with typical AD.

A similar pattern was seen for the 3 patients with atypical AD clinical syndromes. For each patient, [18F]AV-1451 SUVR within a given ROI was strongly correlated with the cortical thickness *z* score (patient 4, $r = -0.51$; $P < .001$; patient 5, $r = -0.63$; $P < .001$; and patient 6, $r = -0.70$; $P < .001$), whereas [11C]PiB tracer uptake was not associated with cortical thickness (patient 4, $r = -0.02$; $P = .89$; patient 5, $r = 0.10$; $P = .44$; and patient 6, $r = 0.06$; $P = .64$). These associations are illustrated in **Figure 4**.

Discussion

The first use of the ligand now known as [18F]AV-1451 in patients with AD was reported in 2013.[25] The selectivity of this ligand for hyperphosphorylated tau was recently confirmed.[26] In addition, a study was completed in which an elevated [18F]AV-1451 signal in mild cognitive impairment likely owing to AD and AD dementia showed a topography largely consistent with Braak staging and its magnitude correlated with level of clinical impairment.[18] In this study, we provide further evidence that clinical phenotype of individual patients with AD is associated with the localization of tau pathologic findings in vivo as measured by [18F]AV-1451 in a series of patients with the typical multidomain amnesic dementia form of AD as well as atypical forms such as PCA, lvPPA, and CBS. Moreover, we demonstrated that the severity of tau pathologic findings measured by the intensity of the [18F]AV-1451 signal within a given cortical ROI is correlated with the magnitude of atrophy. Finally, tau pathologic findings measured by [18F]AV-1451 surpass amyloid pathologic findings measured by [11C]PiB in both association with localization of a given syndrome and in correlating with the degree of atrophy within regions of neurodegeneration.

Our study demonstrates that in individual patients with typical or atypical variant AD, clinical phenotype is associated with the topography of [18F]AV-1451 tracer uptake. This finding provides further in vivo evidence for what has been shown by previous neuropathologic reports demonstrating a strong association between distribution and severity of tau pathologic findings and clinical symptoms in patients with typical and atypical AD,[4] and is also consistent with several recent case reports and one larger study demonstrating a similar pattern of findings.[27-30] The ability of [18F]AV-1451 to localize tau pathologic findings at the individual patient level in a manner concordant with symptoms supports its clinical validity as a new in vivo imaging biomarker in AD. Although cerebrospinal fluid tau has been validated as a specific biomarker of clinically diagnosed and autopsy-confirmed AD,[31] it cannot provide information about the localization of tau pathologic findings. Our ability to test many hypotheses regarding the association of tau to neurologic symptoms in vivo requires information about its localization. Although results of MRI and [18F]FDG-PET imaging are informative regarding the localization of structural or metabolic abnormalities associated with AD pathologic findings,[32,33] they do not provide information regarding the molecular nature of the underlying disease process offered by [18F]AV-1451.

For all patients with AD who were examined in our study, [18F]AV-1451 tracer uptake tightly paralleled cortical atrophy in both localization and severity, again supporting observations from neuropathologic studies indicating a close association between tau pathologic findings and neuronal loss, gliosis, and other evidence of neurodegeneration.[34] Our findings also extend previous case reports and a study that focused mainly on the association between [18F]AV-1451 tracer uptake and hypometabolism measured via [18F]FDG-PET.[27-30] Studies of the pathologic basis of measures of regional atrophy in AD as seen on results of MRI have found associations with neurofibrillary pathologic findings.[33,35] Previous in vivo biomarker investigations in prodromal and mild AD dementia have demonstrated stronger associations between cerebrospinal fluid tau and atrophy in selected temporal cortical regions[36] and in widely distributed cortical regions where thinning is associated with AD.[37] The data presented in Figures 3 and 4 bring these lines of research together, showing that most cortical areas with clear evidence of atrophy (thickness >2 SDs below that of the control group) harbor a substantial burden of tau pathologic findings ([18F]AV-1451 tracer SUVR values >2.0). Conversely, in all the patients, very few cortical regions with [18F]AV-1451 tracer SUVR values above 2.5 do not show obvious atrophy. The strength of these associations may be surprising given that the data from PET imaging were not adjusted for partial volume effects; atrophied ROIs would be expected to reduce the potential dynamic range of the PET signal. As long ago as 1970, Tomlinson et al similarly observed that "severe generalized neurofibrillary change in the cortex was not seen in any control; it seems possible that its occurrence always indicates dementia."[38(p234)] We confirm this association, with evidence linking cortical tau pathologic findings with the in vivo hallmark measure of neurodegeneration—measures of regional atrophy as seen on results of MRI.

Figure 3. Correlations Between Cortical Atrophy and Tau vs Amyloid in Patients With Typical Alzheimer Disease (AD)

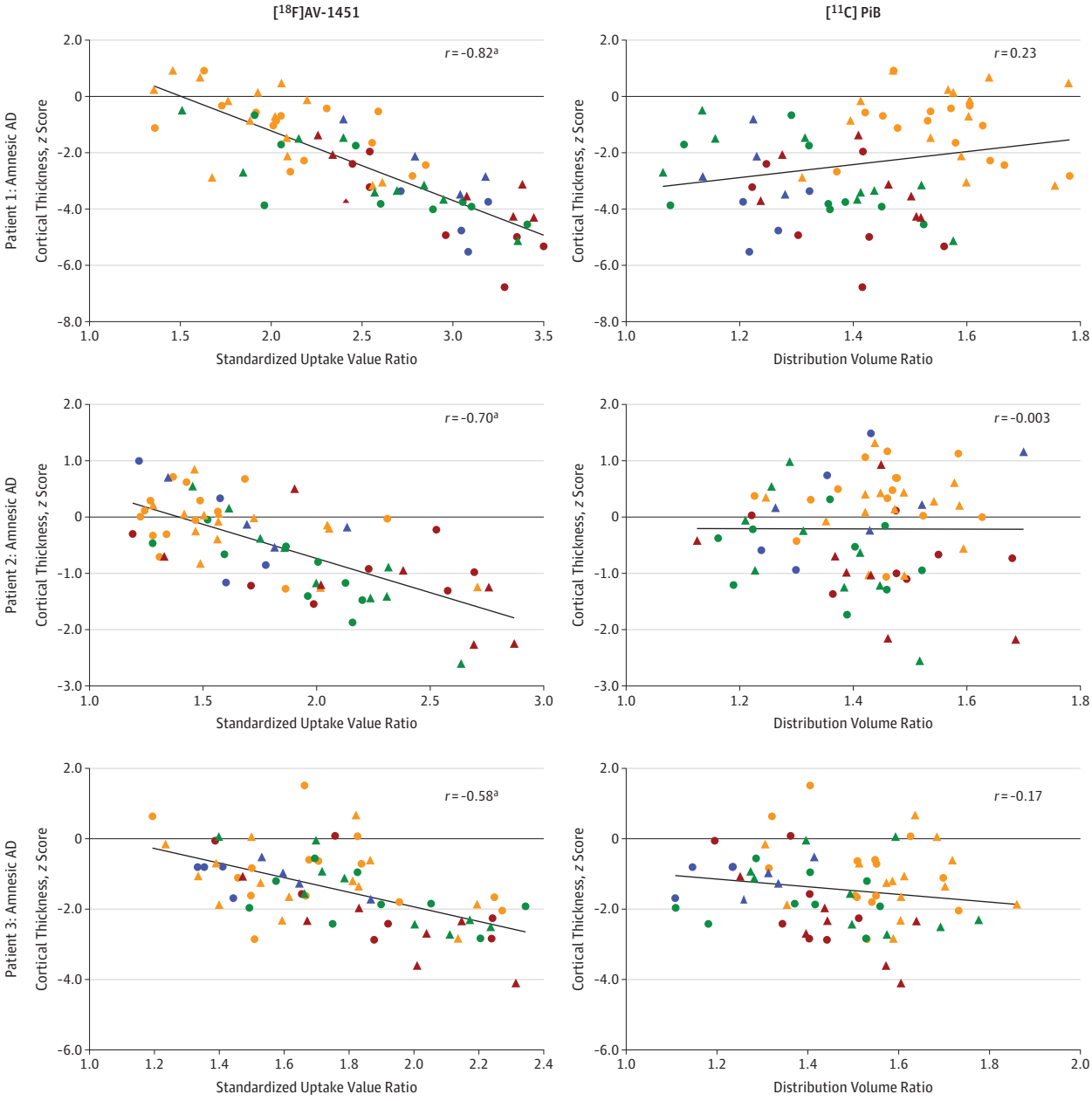

Shapes representing cortical regions of interest: left frontal, amber circles; left temporal, green circles; left parietal, maroon circles; left occipital, blue circles; right frontal, amber triangles; right temporal, green triangles; right parietal, maroon triangles; and right occipital, blue triangles. [11C]PiB indicates carbon 11–labeled Pittsburgh Compound B; [18F]AV-1451, fluorine 18–labeled AV-1451.

a $P < .001$.

In addition to contributing topographic information not obtained from cerebrospinal fluid tau and specifying molecular pathologic findings not provided by structural MRI or [18F]FDG-PET imaging, we showed that tau pathologic findings measured via [18F]AV-1451 also complement [11C]PiB. Amyloid PET imaging has revolutionized AD clinical research since it was first introduced more than a decade ago.[39] However, again as seen in pathologic studies, amyloid imaging studies have failed to show a concordance between the localization and magnitude of the amyloid signal as seen on results of PET imaging with AD clinical symptoms or atrophy and hypometabolism markers of neurodegeneration.[40] Our findings demonstrate that, in patients with typical amnesic AD and those with atypical variant AD, the uptake of [18F]AV-1451 tracer showed distinct topographic patterns associated with specific clinical phenotypes, whereas [11C]PiB did not. We also found that in vivo tau pathologic findings measured via [18F]AV-1451 tracer uptake are associated more closely with topography and the se-

Figure 4. Correlations Between Cortical Atrophy and Tau vs Amyloid in Patients With Atypical Alzheimer Disease

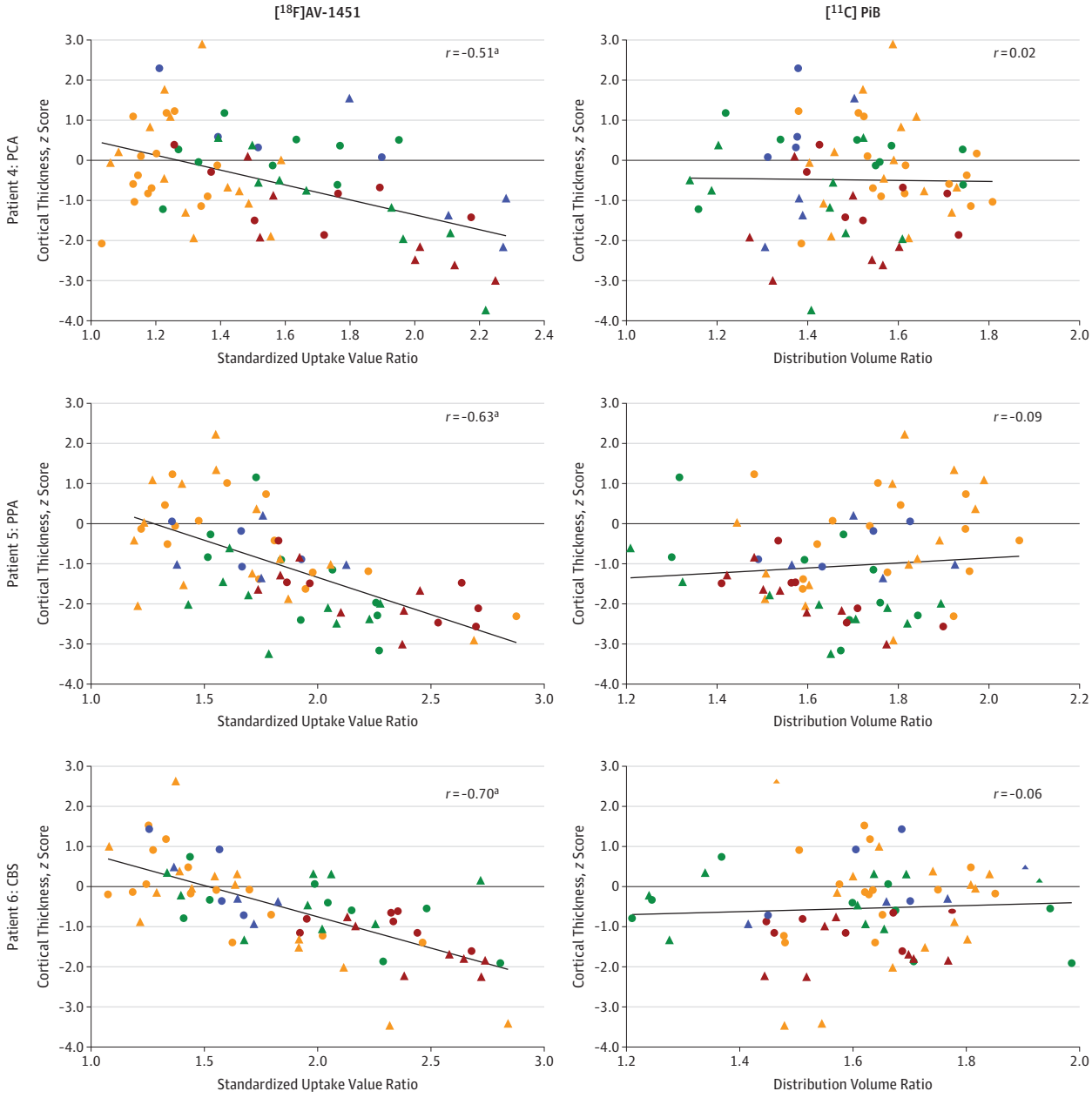

Shapes representing cortical regions of interest: left frontal, amber circles; left temporal, green circles; left parietal, maroon circles; left occipital, blue circles; right frontal, amber triangles; right temporal, green triangles; right parietal, maroon triangles; and right occipital, blue triangles. CBS indicates corticobasal syndrome; [11C]PiB, carbon 11–labeled Pittsburgh Compound B; [18F]AV-1451, fluorine 18–labeled AV-1451; lvPPA, logopenic variant primary progressive aphasia; and PCA, posterior cortical atrophy.

[a] $P < .001$.

verity of cortical atrophy than amyloid pathologic findings measured via [11C]PiB tracer uptake.

Limitations

One limitation of this study is the small number of patients. We did not have a large enough sample size to examine the quantitative association between regional [18F]AV-1451 tracer binding and cognitive measures. This outcome is an aim of a follow-up study. However, given the robustly consistent associations between the measures across all 6 patients with diverse clinical presentations, we are confident that this set of results will be readily replicable in larger samples. Furthermore, the consistency of these results with those of neuropathologic studies provides additional assurance that sample size is not likely a major limitation. Nevertheless, at this point, [18F]AV-1451 PET imaging should be considered an adjunc-

tive tool in the diagnostic evaluation of patients thought to have atypical subtypes of AD; it should be interpreted within the broader clinical context and taking into consideration results from other currently established diagnostic tools.

Conclusions

With this and other emerging evidence of the presence of a substantial [18F]AV-1451 signal in early stages of disease (most patients in this study were in very mild to mild stages of AD dementia), along with its colocalization with other markers of neurodegeneration, [18F]AV-1451 PET imaging may eventually play an important role in the diagnostic evaluation of cases of atypical dementia in clinical practice. Although further studies are needed on the test-retest reliability and longitudinal change of [18F]AV-1451 tracer uptake pattern in association with structural MRI, [18F]FDG-PET imaging, cerebrospinal fluid tau, and amyloid PET imaging, this and other tau ligands of PET imaging will likely add critical momentum to the design of next-generation clinical trials targeting tau pathologic findings.

ARTICLE INFORMATION

Accepted for Publication: December 5, 2016.

Published Online: February 20, 2017. doi:10.1001/jamaneurol.2016.5755

Author Affiliations: Frontotemporal Disorders Unit, Department of Neurology, Massachusetts General Hospital and Harvard Medical School, Charlestown (Xia, Makaretz, Caso, McGinnis, Dickerson); Alzheimer's Disease Research Center, Department of Neurology, Massachusetts General Hospital and Harvard Medical School, Charlestown (Gomperts, Gomez-Isla, Hyman, Johnson, Dickerson); Division of Nuclear Medicine and Molecular Imaging, Department of Radiology, Massachusetts General Hospital and Harvard Medical School, Boston (Sepulcre, Schultz, Vasdev, Johnson); Athinoula A. Martinos Center for Biomedical Imaging, Massachusetts General Hospital and Harvard Medical School, Charlestown (Schultz, Dickerson); Center for Alzheimer Research and Treatment, Department of Neurology, Brigham and Women's Hospital, Boston, Massachusetts (Johnson).

Author Contributions: Dr Dickerson had full access to all the data in the study and takes responsibility for the integrity of the data and the accuracy of the data analysis.
Study concept and design: Johnson, Dickerson.
Acquisition, analysis, or interpretation of data: All authors.
Drafting of the manuscript: Xia, Makaretz, McGinnis, Johnson, Dickerson.
Critical revision of the manuscript for important intellectual content: All authors.
Statistical analysis: Xia, Makaretz, Johnson, Dickerson.
Obtained funding: Hyman, Johnson, Dickerson.
Administrative, technical, or material support: Makaretz, Caso, McGinnis, Johnson, Dickerson.
Study supervision: Hyman, Johnson, Dickerson.

Conflict of Interest Disclosures: Dr Hyman reported receiving personal fees from Siemens, Calico, ISIS Pharma, Eli Lilly, Neurophage Pharmaceuticals, Pfizer, Biogen, Genentech, Sanofi, AbbVie, and Novartis; receving grants from Siemens, Biogen Idec, BMS, AZTherapies, Acumen, Prothena, Fidelity Biosciences, Spark, and Intellect; and having a family member employed by Novartis. Dr Vasdev reported holding patent number WO 2014194169 A1 20141204, "Radiosynthesis of Tau Radio-Pharmaceuticals" (2014). Dr Johnson reported receiving personal fees from Piramal, Novartis, Siemens, Lilly/Avid, Janssen, AZTherapies, Roche, Genentech, GE Healthcare, Biogen Idec, and ISIS Pharma; receiving grants from Lilly/Avid, Merck, Janssen, Eisai, Biogen Idec, the National Institutes of Health, and the Michael J. Fox Foundation. Dr Dickerson reported receiving personal fees from Merck, Forum, and Ionis Pharma. No other disclosures were reported.

Funding/Support: This study was supported by grants R01 AG046396, P01 AG036694, and P50 AG00513421 from the National Institute on Aging, and grants R21 NS079905, R21 NS09024, R21 NS090243 from the National Institute of Neurological Disorders and Stroke, and by Fidelity Biosciences, Harvard Neurodiscovery Center, the Alzheimer's Association, and Fonds de Recherche du Quebec–Sante.

Role of the Funder/Sponsor: The funding sources were not involved in the design and conduct of the study; collection, management, analysis, and interpretation of the data; preparation, review, or approval of the manuscript; and decision to submit the manuscript for publication.

Additional Contributions: We thank the patients and families who participated in this study, and the staff involved in coordinating study visits and assessments.

REFERENCES

1. Galton CJ, Patterson K, Xuereb JH, Hodges JR. Atypical and typical presentations of Alzheimer's disease: a clinical, neuropsychological, neuroimaging and pathological study of 13 cases. *Brain*. 2000;123(pt 3):484-498.

2. Montine TJ, Phelps CH, Beach TG, et al; National Institute on Aging; Alzheimer's Association. National Institute on Aging–Alzheimer's Association guidelines for the neuropathologic assessment of Alzheimer's disease: a practical approach. *Acta Neuropathol*. 2012;123(1):1-11.

3. Arriagada PV, Growdon JH, Hedley-Whyte ET, Hyman BT. Neurofibrillary tangles but not senile plaques parallel duration and severity of Alzheimer's disease. *Neurology*. 1992;42(3, pt 1):631-639.

4. Nelson PT, Alafuzoff I, Bigio EH, et al. Correlation of Alzheimer disease neuropathologic changes with cognitive status: a review of the literature. *J Neuropathol Exp Neurol*. 2012;71(5):362-381.

5. Wolk DA. Amyloid imaging in atypical presentations of Alzheimer's disease. *Curr Neurol Neurosci Rep*. 2013;13(12):412.

6. Hof PR, Bouras C, Constantinidis J, Morrison JH. Balint's syndrome in Alzheimer's disease: specific disruption of the occipito-parietal visual pathway. *Brain Res*. 1989;493(2):368-375.

7. Johnson JK, Head E, Kim R, Starr A, Cotman CW. Clinical and pathological evidence for a frontal variant of Alzheimer disease. *Arch Neurol*. 1999;56(10):1233-1239.

8. Gefen T, Gasho K, Rademaker A, et al. Clinically concordant variations of Alzheimer pathology in aphasic versus amnestic dementia. *Brain*. 2012;135(pt 5):1554-1565.

9. Villemagne VL, Fodero-Tavoletti MT, Masters CL, Rowe CC. Tau imaging: early progress and future directions. *Lancet Neurol*. 2015;14(1):114-124.

10. Sapolsky D, Bakkour A, Negreira A, et al. Cortical neuroanatomic correlates of symptom severity in primary progressive aphasia. *Neurology*. 2010;75(4):358-366.

11. McKhann GM, Knopman DS, Chertkow H, et al. The diagnosis of dementia due to Alzheimer's disease: recommendations from the National Institute on Aging-Alzheimer's Association workgroups on diagnostic guidelines for Alzheimer's disease. *Alzheimers Dement*. 2011;7(3):263-269.

12. Mendez MF, Ghajarania M, Perryman KM. Posterior cortical atrophy: clinical characteristics and differences compared to Alzheimer's disease. *Dement Geriatr Cogn Disord*. 2002;14(1):33-40.

13. Crutch SJ, Schott JM, Rabinovici GD, et al. Shining a light on posterior cortical atrophy. *Alzheimers Dement*. 2013;9(4):463-465.

14. Gorno-Tempini ML, Hillis AE, Weintraub S, et al. Classification of primary progressive aphasia and its variants. *Neurology*. 2011;76(11):1006-1014.

15. Armstrong MJ, Litvan I, Lang AE, et al. Criteria for the diagnosis of corticobasal degeneration. *Neurology*. 2013;80(5):496-503.

16. Shoup TM, Yokell DL, Rice PA, et al. A concise radiosynthesis of the tau radiopharmaceutical, [18F]T807. *J Labelled Comp Radiopharm*. 2013;56(14):736-740.

17. Wilson AA, Garcia A, Chestakova A, et al. A rapid one-step radiosynthesis of the β-amyloid imaging radiotracer *N*-methyl-[11C]2-(4'-methylaminophenyl)-6-hydroxybenzothiazole([11C]-6-OH-BTA-1). *J Labelled Comp Radiopharm*. 2004;47:679-682. doi:10.1002/jlcr.854

18. Johnson KA, Schultz A, Betensky RA, et al. Tau positron emission tomographic imaging in aging and early Alzheimer disease. *Ann Neurol*. 2016;79(1):110-119.

19. Becker JA, Hedden T, Carmasin J, et al. Amyloid-β associated cortical thinning in clinically normal elderly. *Ann Neurol*. 2011;69(6):1032-1042.

20. Logan J, Fowler JS, Volkow ND, et al. Graphical analysis of reversible radioligand binding from time-activity measurements applied to

[*N*-11C-methyl]-(–)-cocaine PET studies in human subjects. *J Cereb Blood Flow Metab*. 1990;10(5):740-747.

21. Dickerson BC, Fenstermacher E, Salat DH, et al. Detection of cortical thickness correlates of cognitive performance: reliability across MRI scan sessions, scanners, and field strengths. *Neuroimage*. 2008;39(1):10-18.

22. Desikan RS, Ségonne F, Fischl B, et al. An automated labeling system for subdividing the human cerebral cortex on MRI scans into gyral based regions of interest. *Neuroimage*. 2006;31(3):968-980.

23. Braak H, Braak E. Neuropathological stageing of Alzheimer-related changes. *Acta Neuropathol*. 1991;82(4):239-259.

24. Klunk WE, Engler H, Nordberg A, et al. Imaging brain amyloid in Alzheimer's disease with Pittsburgh Compound-B. *Ann Neurol*. 2004;55(3):306-319.

25. Chien DT, Bahri S, Szardenings AK, et al. Early clinical PET imaging results with the novel PHF-tau radioligand [F-18]-T807. *J Alzheimers Dis*. 2013;34(2):457-468.

26. Marquié M, Normandin MD, Vanderburg CR, et al. Validating novel tau positron emission tomography tracer [F-18]-AV-1451 (T807) on postmortem brain tissue. *Ann Neurol*. 2015;78(5):787-800.

27. Smith R, Wibom M, Olsson T, et al. Posterior accumulation of tau and concordant hypometabolism in an early-onset Alzheimer's disease patient with presenilin-1 mutation. *J Alzheimers Dis*. 2016;51(2):339-343.

28. Pascual B, Masdeu JC. Tau, amyloid, and hypometabolism in the logopenic variant of primary progressive aphasia. *Neurology*. 2016;86(5):487-488.

29. Ossenkoppele R, Schonhaut DR, Schöll M, et al. Tau PET patterns mirror clinical and neuroanatomical variability in Alzheimer's disease. *Brain*. 2016;139(pt 5):1551-1567.

30. Ossenkoppele R, Schonhaut DR, Baker SL, et al. Tau, amyloid, and hypometabolism in a patient with posterior cortical atrophy. *Ann Neurol*. 2015;77(2):338-342.

31. Shaw LM, Vanderstichele H, Knapik-Czajka M, et al; Alzheimer's Disease Neuroimaging Initiative. Cerebrospinal fluid biomarker signature in Alzheimer's disease neuroimaging initiative subjects. *Ann Neurol*. 2009;65(4):403-413.

32. Silverman DHS, Small GW, Chang CY, et al. Positron emission tomography in evaluation of dementia: regional brain metabolism and long-term outcome. *JAMA*. 2001;286(17):2120-2127.

33. Silbert LC, Quinn JF, Moore MM, et al. Changes in premorbid brain volume predict Alzheimer's disease pathology. *Neurology*. 2003;61(4):487-492.

34. Gómez-Isla T, Hollister R, West H, et al. Neuronal loss correlates with but exceeds neurofibrillary tangles in Alzheimer's disease. *Ann Neurol*. 1997;41(1):17-24.

35. Whitwell JL, Josephs KA, Murray ME, et al. MRI correlates of neurofibrillary tangle pathology at autopsy: a voxel-based morphometry study. *Neurology*. 2008;71(10):743-749.

36. Desikan RS, McEvoy LK, Thompson WK, et al; Alzheimer's Disease Neuroimaging Initiative. Amyloid-β associated volume loss occurs only in the presence of phospho-tau. *Ann Neurol*. 2011;70(4):657-661.

37. Dickerson BC, Wolk DA; Alzheimer's Disease Neuroimaging Initiative. Biomarker-based prediction of progression in MCI: Comparison of AD signature and hippocampal volume with spinal fluid amyloid-β and tau. *Front Aging Neurosci*. 2013;5:55.

38. Tomlinson BE, Blessed G, Roth M. Observations on the brains of demented old people. *J Neurol Sci*. 1970;11(3):205-242.

39. Johnson KA, Minoshima S, Bohnen NI, et al. Guidelines for brain amyloid imaging published. *J Nucl Med*. 2013;54:476-490.

40. Wolk DA, Price JC, Madeira C, et al. Amyloid imaging in dementias with atypical presentation. *Alzheimers Dement*. 2012;8(5):389-398.